IEEE Access
Multidisciplinary | Rapid Review | Open Access Journal

Received 4 January 2023, accepted 17 January 2023, date of publication 23 January 2023, date of current version 27 January 2023.

Digital Object Identifier 10.1109/ACCESS.2023.3239420

RESEARCH ARTICLE

Reconnection-Less Reconfigurable Filter Based on Method of Unknown Nodal Voltages Using 4 × 4 Matrix

LUKAS LANGHAMMER[1,2] AND ROMAN SOTNER[2], (Member, IEEE)
[1]Department of Electrical Engineering, Faculty of Military Technology, University of Defence, 60200 Brno, Czech Republic
[2]Faculty of Electrical Engineering and Communication, Brno University of Technology, 61600 Brno, Czech Republic

Corresponding author: Lukas Langhammer (lukas.langhammer@unob.cz)

This work was supported by the Infrastructure of the Department of Electronics, University of Defence, Brno.

ABSTRACT The paper introduces a novel design solution of a reconnection-less reconfigurable filter based on the method of unknown nodal voltages (MUNV). The filter offers all standard 2nd-order transfer functions and the electronic adjustment of the pole frequency and quality factor, which are mutually independent. The introduced design brings following advantages in comparison to other relevant solutions (MUNV-based reconnection-less reconfigurable filters): a) it consists of four independent nodes which brings the advantage of both working capacitors being grounded as floating capacitors can cause unpredictable parasitic behavior, b) the additional adjustment of the quality factor, c) the additional adjustment of the pass-band at lower and higher frequencies. Simulations and experimental measurements were carried out in order to verify the proposed design.

INDEX TERMS Electronic adjustment, frequency filter, method of unknown nodal voltages, operational transconductance amplifier, reconnection-less reconfiguration.

I. INTRODUCTION

Commonly proposed analogue frequency filters which provide several transfer functions [1], [2], [3], [4], [5], [6], [7], [8], [9], [10], [11] have multiple inputs and/or outputs. Typical topologies (organization of inputs and outputs) are known as: Single-Input Multiple-Output (SIMO) filters [1], [2], [3], Multiple-Input Single-Output filters [4], [5], [6], [7], [8] and Multiple-Input Multiple-Output (MIMO) filters [9], [10], [11]. Specific type of the transfer function is then available based on the selection of input/output (or a suitable combination of inputs/outputs). That brings necessity of switching between these inputs/outputs of above-mentioned filtering topologies. Otherwise, (when the filter has one input and one output), the modification of the inner topology (interconnections of passive and active elements) is required for transfer response change. These actions are typically not possible in case of the on-chip implementation. The switching (of the inputs/outputs) can be achieved through electronically controllable switches. Nonetheless, it can bring additional possible issues such as extra required chip area for the switching logic, necessity to properly design the digital control including a possible requirement of decoders, potential interference caused by the switching process affecting other parts of the application (leakage of distortion from control logic), additional parasitic effects of the switches (finite ON resistance, capacity in OFF state, possible signal level limitation, etc.), variation of input/output impedance regarding matched load (further processing blocks), etc.

The solution of the above-described problem is the utilization of so-called reconnection-less reconfigurable (switchless) filters [12], [13], [14], [15], [16], [17], [18], [19], [20], [21] where the change of the transfer functions does not require any switching or topological changes. The general concept comes from the frequency filters operating in the microwave systems [12], [13], [14], [15] where the reconfiguration of the transfer function has its origin in the electromagnetic coupling of elements. The low-frequency (up to hundreds of megahertz) filters [16], [17], [18], [19], [20], [21] implement the reconnection-less reconfiguration

The associate editor coordinating the review of this manuscript and approving it for publication was Sai-Weng Sin.

TABLE 1. Comparison of reconnection-less reconfigurable filters based on MUNV.

Reference	Number of active/passive elements	Available transfer functions	Type of active elements	Simulated/measured	Fully independent adjustment of quality factor	Grounded capacitors	Additional adjustment of quality factor	Additional adjustment of pass-band area
[16]	4/2	AP, BP, BS, HP, HPZ, LPZ	OTA	Yes/No	No	No	No	No
	4/2	AP, BP, BS, HP, HPZ, LPZ	OTA	Yes/No	No	No	No	No
[17]	4/2	AP, BP, BS	OTA	Yes/No	Yes	No	No	No
	4/3	AP, BP, BS, HP, HPZ, LPZ	OTA	Yes/No	No	No	No	No
[18]	3 (5)[1]/2	AP, BS, LP, LPZ, 1st-order HP, DT	VDTA (OTA), VGA	Yes/No	Yes	Partly[2]	No	No
[19]	4/2	AP, BS, HP, HPZ, 1st-order HP, DT	OTA, VGA	Yes/No	No	No	No	No
Fig. 2	8/2	AP, BP, BS, HP, HPZ, LP, LPZ	OTA	Yes/Yes	Yes	Yes	Yes	Yes

Notes:
[1]the filter is built by two VDTAs (each created by two OTAs) and one VGA, [2]one of the capacitors is virtually grounded through the voltage (low impedance) output of the VGA.

by the utilization of electronically controllable active elements (the transfer function is changed by the setting of electronically controllable parameters of active elements employed in given topology). The electromagnetic coupling would be difficult to implement at these frequencies. Filters presented in works [16], [17], [18], [19] are created by the Method of Unknown Nodal Voltages (MUNV) [22]. The same approach has been used for the presented design. Other common approach for the design of reconnection-less reconfigurable filters, used for filters in [20] and [21], is done by Signal Flow Graphs (SFGs) [23] (combination of Mason graphs [24] and Coates graphs [25] is typically used). The design in [16] is based on four Operational Transconductance Amplifiers (OTAs) with one grounded and one floating capacitor. It provides standard 2nd-order functions (all-pass (AP), high-pass (HP), low-pass (LP), band-pass (BP) and band-stop (BS) functions) excluding LP function. The design also offers high-pass and low-pass functions with zero in their transfer (HPZ and LPZ). The design is supported by simulation results. Reference [17] is offering three solutions each based on four OTAs one grounded and one floating capacitor. One of the solutions additionally contains a resistor. The first and third solution offer AP, HP, BP, BS, HPZ and LPZ functions. The second solution provides AP, BP and BS functions. Furthermore, the second solution offers the fully independent adjustment of the quality factor. The function of the first solution was verified by simulations. The structure in [18] consists of two Voltage Differencing Transconductance Amplifiers (VDTAs), one Variable Gain Amplifier (VGA), one grounded capacitor and one virtually grounded capacitor (grounded through the voltage (low-impedance) output of the VGA). Functions of AP, BS, LP, LPZ, 1st-order HP and direct transfer (DT) are available. The filter offers the fully independent adjustment of the quality factor. Simulation results are provided. The filter in [19] is also based on two types of active elements (OTA and VGA) with one grounded capacitor and one floating capacitor. The topology provides functions of AP, BS, HP, HPZ, 1st-order HP and DT. The design is supported by simulation results. A comparison of previously proposed reconnection-less reconfigurable filters (based on MUNV) in relation to the newly introduced proposal is provided in Table 1. Based on the study of Table 1, the following conclusions can be stated:

- The proposed filter is using unified type of the active element in comparison to [18] and [19], where two different types are required for the function.
- All previous solutions are verified only by simulations unlike the proposed filter which is also supported by experimental measurements.
- Except for the proposed filter, only solution in [18] and specific topology from reported solutions in [17] offer the fully independent electronic control of the quality factor.
- Neither of the filters in Table 1, except for the solution proposed in this paper, can operate with both working capacitors grounded.
- The proposed filter offers feature of an additional adjustment of the quality factor.
- The proposed filter offers feature of an additional adjustment of the pass-band range at lower and higher frequencies.
- The proposed filter requires higher number of used active elements than other solutions. Nonetheless, these additional active elements bring new features available simultaneously (independent electronic control of the quality factor, additional control of the quality factor and additional adjustment of the pass-band area at lower and higher frequencies).

The design solution of the reconnection-less reconfigurable filter presented in this paper uses the MUNV 4 × 4 matrix. It results into both working grounded capacitors in the topology in comparison to previously proposed reconnection-less reconfigurable filters based on MUNV. The filter offers all standard 2nd-order transfer functions available

through the reconnection-less reconfiguration. The independent electronic adjustment of the pole frequency and quality factor is available. Moreover, the proposed filter offers the additional adjustment of the quality factor and the additional adjustment of the pass-band area at lower and higher frequencies. The function of the filter is verified by PSpice simulations and experimental measurements using commercially available devices.

The organization of the paper is following: Chapter I discusses the topic associated with the proposed filtering topology. Chapter II explains the design procedure, used active element principle and the general features of the proposed filter. The verification of the circuit in form of simulation and experimental results demonstrating available features is provided in Chapter III. The paper is concluded in Chapter IV.

II. DESIGN PROPOSAL

All previously proposed (MUNV-based) reconnection-less reconfigurable filters [16], [17], [18], [19] have an inherent disadvantage - one working capacitor is floating due to the design established on 3 × 3 admittance matrix (proposed circuit having 3 independent nodes). Floating capacitors are generally not suitable for the on-chip implementation as they can cause unpredictable parasitic behavior [26]. The usage of 3 × 3 matrix in [16], [17], [18], [19] has been done due to the increasing complexity of the mathematical expression of the algebraic complements for Laplace expansion of the sub-determinants if the matrix dimensions are higher than 3 × 3. Nonetheless, the mathematical expression of 4 × 4 (and higher) matrix is possible and (if designed properly) it brings the advantage of both nodal working capacitors of grounded connection. It eliminates the disadvantages of previously proposed MUNV-based solutions.

The design supposes the utilization of Operational Transconductance Amplifiers (OTAs) [27] as the active element. The OTA principle (in the ideal case) is identical to a voltage controlled current source. The schematic symbol and used implementation of the OTA by real element is shown in Fig. 1. The OTA consists of two voltage inputs (of opposite polarity – differential input) and one current output. Its behavior is described by the relation $I_{out} = g_m \cdot (V_{in+} - V_{in-})$, where g_m denotes the transconductance of this active element. The real implementation is created by LT1228 device [28], which is commercially available. The LT1228 consists of OTA part and CFA part while the CFA is not being used in our case. Fig. 1b) shows a complete connection of the LT1228 (including the pin numbers of the chip). The value of the transconductance in dependence on control DC voltage V_{SET_gm} is given by relation (1).

$$g_m \cong 10 \cdot \frac{V_{SET\_gm} + |V_{SS}| - 1.4}{R} \tag{1}$$

The design considers following rules: the filter has four independent nodes (leading to 4 × 4 matrix), the filter has one input and one output (Single-Input Single-Output filter type) to fulfill the condition of the reconnection-less

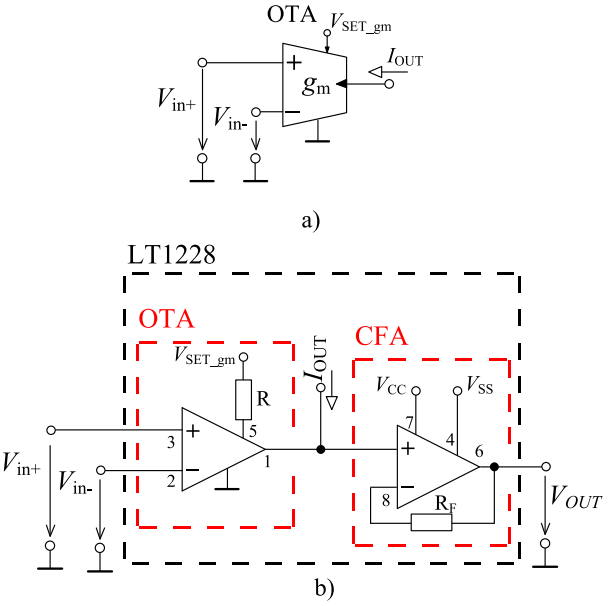

FIGURE 1. Operational Transconductance Amplifier (OTA): a) schematic symbol, b) implementation of the OTA using the LT1228 device.

reconfiguration, the excitation source is connected to node 1 and node 4 is considered to be the output of the filter. Based on these facts, the general MUNV matrix takes the following form:

$$\begin{pmatrix} Y_{11} & Y_{12} & Y_{13} & Y_{14} \\ Y_{21} & Y_{22} & Y_{23} & Y_{24} \\ Y_{31} & Y_{32} & Y_{33} & Y_{34} \\ Y_{41} & Y_{42} & Y_{43} & Y_{44} \end{pmatrix} \cdot \begin{pmatrix} V_1 \\ V_2 \\ V_3 \\ V_4 \end{pmatrix} = \begin{pmatrix} I_1 \\ 0 \\ 0 \\ 0 \end{pmatrix}. \tag{2}$$

Supposing $K(s) = N(s)/D(s) = V_{OUT}/V_{IN} = V_4/V_1 = \Delta_{1,4}/\Delta_{1,1}$, where:

$$\begin{aligned} \Delta_{1,1} &= Y_{22}Y_{33}Y_{44} - Y_{22}Y_{34}Y_{43} - Y_{23}Y_{32}Y_{44} \\ &\quad + Y_{23}Y_{34}Y_{42} + Y_{24}Y_{32}Y_{43} - Y_{24}Y_{33}Y_{42} \\ &= b_2 s^2 + b_1 s + b_0, \end{aligned} \tag{3}$$

$$\begin{aligned} \Delta_{1,4} &= Y_{21}Y_{32}Y_{43} - Y_{21}Y_{33}Y_{42} - Y_{22}Y_{31}Y_{43} \\ &\quad + Y_{22}Y_{33}Y_{41} + Y_{23}Y_{31}Y_{42} - Y_{23}Y_{32}Y_{41} \\ &= a_2 s^2 + a_1 s + a_0. \end{aligned} \tag{4}$$

The steps of the design are following:

1) Each term (product of three admittances) in (3) and (4) will be creating one coefficient (s^2, s^1 and s^0) of the resulting transfer function. Since each sub-determinant consists of six terms, three of them (three in (3) and three in (4)) must be canceled.
2) C_1 is connected (initial selection) to node 2 and C_2 is connected to node 3. Both capacitors are grounded. That way $Y_{22}Y_{33}Y_{44}$ in (3) creates s^2 term in the denominator (D) and $Y_{22}Y_{33}Y_{41}$ in (4) defines s^2 term in the numerator (N).
3) Based on 2), there are two s^1 terms ($-Y_{22}Y_{34}Y_{43}$ and $-Y_{24}Y_{33}Y_{42}$) in (3) and two ($-Y_{21}Y_{33}Y_{42}$ and $-Y_{22}Y_{31}Y_{43}$) in (4). Since we need only one s^1 term

in (N) and one in (D), it has been decided that $Y_{42} = 0$ (open). It cancels terms $Y_{23}Y_{34}Y_{42}$ and $-Y_{24}Y_{33}Y_{42}$ in (3) and terms $-Y_{21}Y_{33}Y_{42}$ and $Y_{23}Y_{31}Y_{42}$ in (4).

4) There are still two $\mathbf{s}^0$ terms (produced by $-Y_{23}Y_{32}Y_{44}$ and $Y_{24}Y_{32}Y_{43}$) remaining in (3) and two $\mathbf{s}^0$ terms (produced by $Y_{21}Y_{32}Y_{43}$ and $-Y_{23}Y_{32}Y_{41}$) remaining in (4). Either Y_{23} or Y_{21} together with Y_{24} must be set to zero (other parameters appear in different terms and thus cannot be set to zero). It has been chosen that $Y_{23} = 0$.
5) The pole frequency f_0 has been determined to be adjusted by transconductances g_{m1} and g_{m2} thus, $Y_{32} = g_{m1}$ and $Y_{43} = g_{m2}$. The quality factor Q is going to be adjusted by g_{m3}, therefore, $Y_{43} = g_{m3}$. Furthermore (for reconnection-less reconfigurability purposes), it has been decided s^0 term in (N) can be adjusted by g_{m4}, s^1 term in (N) can be adjusted by g_{m5} and s^2 term in (N) can be adjusted by g_{m6}. Since Y_{44} and Y_{24} cannot be zero then $Y_{24} = g_{m7}$ and $Y_{44} = g_{m8}$.
6) After the selection of parameters for various adjustments and reconfiguration, polarities of individual parameters have to be ensured in accordance with (3) and (4). All terms in (D) must be positive. s^2 and s^0 term in (N) must be positive while s^1 term of (N) is negative, or vice versa (depending on whether we want to obtain inverting or non-inverting polarities of output responses). Thus, the polarities have been selected as follows: $Y_{32} = g_{m1}$, $Y_{43} = -g_{m2}$, $Y_{34} = g_{m3}$, $Y_{21} = -g_{m4}$, $Y_{31} = -g_{m5}$, $Y_{41} = g_{m6}$, $Y_{24} = -g_{m7}$ and $Y_{44} = g_{m8}$.

Based on these steps, the resulting relations (3) (the denominator) and (4) (the numerator) turn into:

$$\begin{aligned}\Delta_{1,1} = D(s) &= Y_{22}Y_{33}Y_{44} - Y_{22}Y_{34}Y_{43} + Y_{24}Y_{32}Y_{43}\\ &= sC_1 \cdot sC_2 \cdot g_{m8} - (sC_1 \cdot g_{m3} \cdot (-g_{m2}))\\ &\quad + g_{m1} \cdot (-g_{m2}) \cdot (-g_{m7})\\ &= s^2C_1C_2g_{m8} + sC_1g_{m2}g_{m3} + g_{m1}g_{m2}g_{m7}, \qquad (5)\\ \Delta_{1,4} = N(s) &= Y_{21}Y_{32}Y_{43} - Y_{22}Y_{31}Y_{43} + Y_{22}Y_{33}Y_{41}\\ &= g_{m1} \cdot (-g_{m2}) \cdot (-g_{m4}) - (sC_1 \cdot (-g_{m5}) \cdot (-g_{m2}))\\ &\quad + sC_1 \cdot sC_2 \cdot g_{m6}\\ &= s^2C_1C_2g_{m6} - sC_1g_{m2}g_{m5} + g_{m1}g_{m2}g_{m4}. \qquad (6)\end{aligned}$$

The resulting matrix of the proposed reconnection-less reconfigurable filter (cells in the first row are zeros as they are not worked with when calculating sub-determinants $\Delta_{1,4}$ and $\Delta_{1,1}$) has the form of:

$$\begin{pmatrix} 0 & 0 & 0 & 0\\ -g_{m4} & sC_1 & 0 & -g_{m7}\\ -g_{m5} & g_{m1} & sC_2 & g_{m3}\\ g_{m6} & 0 & -g_{m2} & g_{m8}\end{pmatrix} \cdot \begin{pmatrix} V_1\\ V_2\\ V_3\\ V_4\end{pmatrix} = \begin{pmatrix} I_1\\ 0\\ 0\\ 0\end{pmatrix}. \qquad (7)$$

The topology of the proposed filter (Fig. 2) can be directly synthesized from the matrix (7). The filter consists of eight

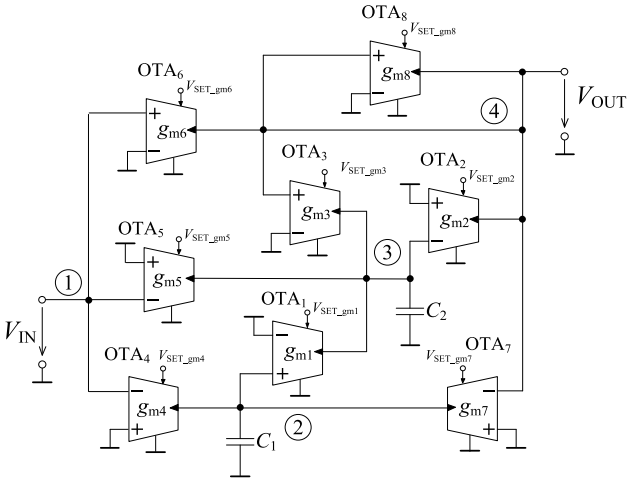

FIGURE 2. Proposed reconnection-less reconfigurable filter based on 4 × 4 MUNV matrix.

OTAs and two capacitors (both grounded). Its transfer function is given as:

$$K(s) = \frac{N(s)}{D(s)} = \frac{s^2C_1C_2g_{m6} - sC_1g_{m2}g_{m5} + g_{m1}g_{m2}g_{m4}}{s^2C_1C_2g_{m8} + sC_1g_{m2}g_{m3} + g_{m1}g_{m2}g_{m7}}. \qquad (8)$$

The filter requires 8 active elements in comparison to previously proposed MUNV based filters (4 active elements for [16], [17], and [19] and 5 active elements for [18]) which could be considered as a disadvantage. Nevertheless, the higher number of active elements brings additional degrees of adjustment: OTA_3 (g_{m3}) provides the independent adjustment of the quality factor and OTA_7 (g_{m7}) and OTA_8 (g_{m8}) offer an additional adjustment of the pass-band area at lower/higher frequencies and also an additional adjustment of the quality factor (as shown later). The setting of g_{m4}, g_{m5} and g_{m6} defines the features of the reconnection-less reconfiguration. Equations (9) and (10) express the relations for the pole frequency f_0 and quality factor Q.

The pole frequency can be adjusted by transconductances g_{m1} and g_{m2} with no effect on the quality factor (when a simple condition $g_{m1} = g_{m2}$ is fulfilled). The quality factor can be adjusted by g_{m3} without impact on the value of the pole frequency. Furthermore, thanks to the specific topology design, the value of the quality factor can be also adjusted by transconductances g_{m7} and g_{m8} as long as they are equal to each other (so they do not affect the value of f_0). The resulting change of the pass-band level caused by the change g_{m7} and g_{m8} can be easily compensated by g_{m4} and g_{m6}. C_1 and C_2 could be used for the adjustment of f_0 or Q, but they would have to be replaced for any change of f_0 or Q which is not possible in case of on-chip implementation, for instance. The capacitors could be replaced by capacitance multipliers in order to obtain the electronic adjustment, but that would increase the circuit complexity. Other additional adjustment of f_0 could be done by the change of g_{m7} and g_{m8}. Nonetheless, a condition $g_{m7} \cdot n$ and g_{m8}/n (or vice versa),

TABLE 2. Settings of reconnection-less reconfigurable feature based on the desired output function.

Function	g_{m4} [mS]	g_{m5} [mS]	g_{m6} [mS]
LP	1	0	0
BP	0	1	0
HP	0	0	1
BS	1	0	1
AP	1	1	1
LPZ	1	0	> 0
HPZ	> 0	0	1

where n is a real positive number would have to be fulfilled so Q is not affected. Additionally, the gain change caused by the adjustment of g_{m7} and g_{m8} would have to be compensated by g_{m4} and g_{m6}. Similarly, the adjustment of Q could be also done by the change of g_{m1} and g_{m2}. In such case, a condition $g_{m1} \cdot n$ and g_{m2}/n (or vice versa) would have to be fulfilled so the tuning process does not affect the value of f_0. The resulting transfer functions (configured responses), based on the setting of g_{m4}, g_{m5} and g_{m6}, are provided in Table 2.

$$f_0 = \frac{1}{2\pi}\sqrt{\frac{g_{m1}g_{m2}g_{m7}}{C_1C_2g_{m8}}} \tag{9}$$

$$Q = \frac{1}{g_{m3}}\sqrt{\frac{C_2g_{m1}g_{m7}g_{m8}}{C_1g_{m2}}} \tag{10}$$

III. SIMULATION AND EXPERIMENTAL RESULTS

The design of the filter has been verified by PSpice simulations and experimental measurements. Simulations were performed using available macro-models of LT1228 while the measurements were done with help of the Agilent 4395A network analyzer using LT1228 devices as presented in the previous section. Fig. 3 shows the implemented printed circuit board (PCB) of the filter. Fig. 4 (top) depicts the block diagram of the measurement setup and Fig. 4 (bottom) shows the photo of the measurement workplace while measuring the proposed filter (when set for BS response). The PCB and the analyzer are interconnected by standard BNC cables. A proper calibration of the signal path has been done before the measurement in order to eliminate the parasitic characteristics of the cables. The analyzer has been set to measure in range from 100 Hz to 100 MHz with 501 points (83 points per decade) with −20 dBm source level. A bench power supply has been used for the supply of active elements and the adjustment of individual transconductances. The setup of the values of individual parameters of the initial state is following: $C_1 = C_2 = 1$ nF, $g_{m1} = g_{m2} = g_{m3} = g_{m7} = g_{m8} = 1$ mS, g_{m4}, g_{m5} and g_{m6} are set in accordance to Table 2 depending on the selected resulting function. These values determine the theoretical pole frequency $f_0 = 159.2$ kHz and quality factor $Q = 1$.

Simulation results are presented by black dashed lines and the experimental results are denoted by colored lines.

Fig. 5 depicts magnitude and phase characteristics of available functions of LP, BP, HP and BS while Fig. 6 shows the

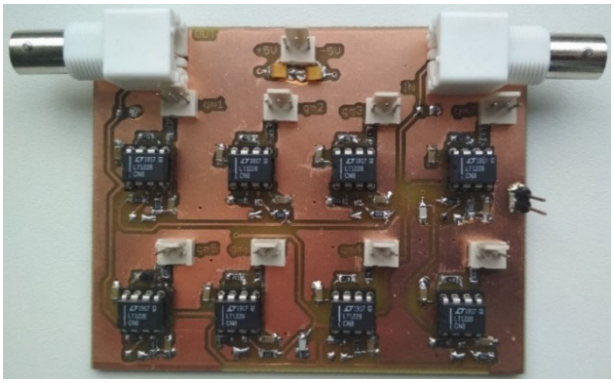

FIGURE 3. Experimental PCB of the proposed filter.

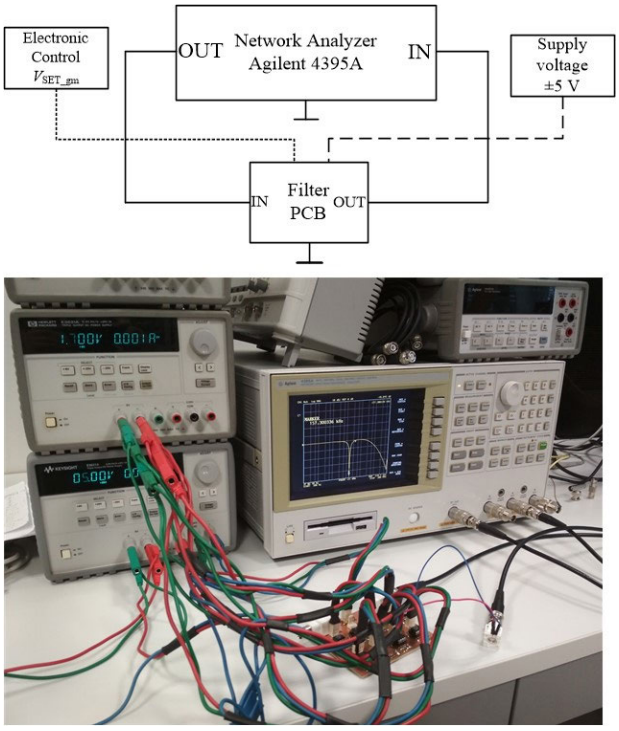

FIGURE 4. Block diagram of the measurement setup (top), measurement workplace – currently measuring BS function (bottom).

characteristic responses (magnitude, phase and group delay) of the available AP function. It can be seen that the filter function is appropriate and usable up to approximately 2 MHz (in case of measurement) due to real properties of the used implementation of the OTAs and designed PCB. Therefore, the design is more suitable for lower frequencies (e.g. usage for acoustic or medical purposes). The measured results are affected by the parasitic/real characteristics of LT1228 device used for the implementation. Based on the datasheet [28], the impedance of the voltage inputs (of the OTA part inside LT1228) is 1 GΩ and 3 pF while the impedance of the current output is stated as 8 MΩ and 6 pF. These impedances affect the stop–band area of available transfer functions (the magnitude trace does not follow the theoretical slope of attenuation but stays at specific value of attenuation). Similarly, the

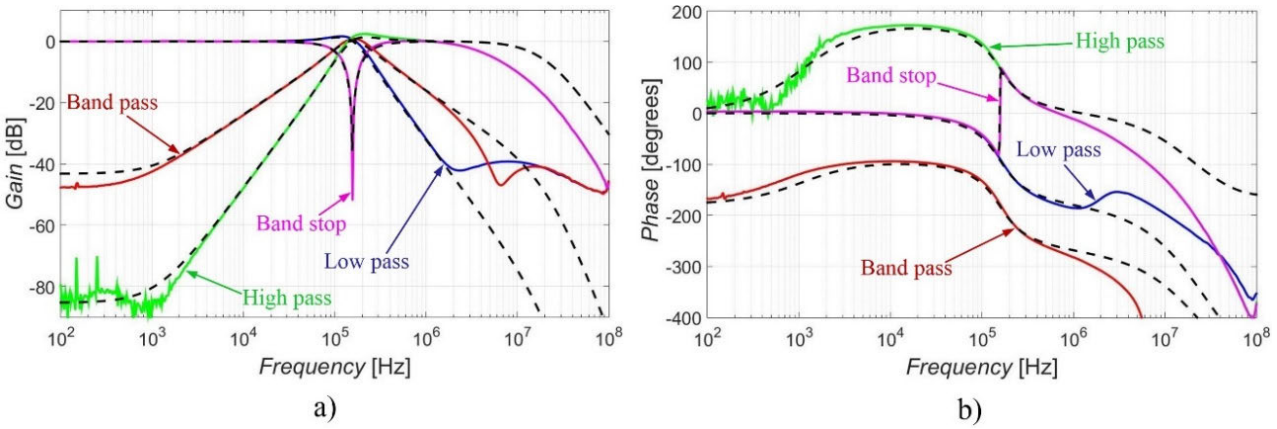

FIGURE 5. Simulation (black dashed lines) and experimental results (colored lines) of LP, BP, HP and BS functions: a) magnitude characteristics and b) phase characteristics.

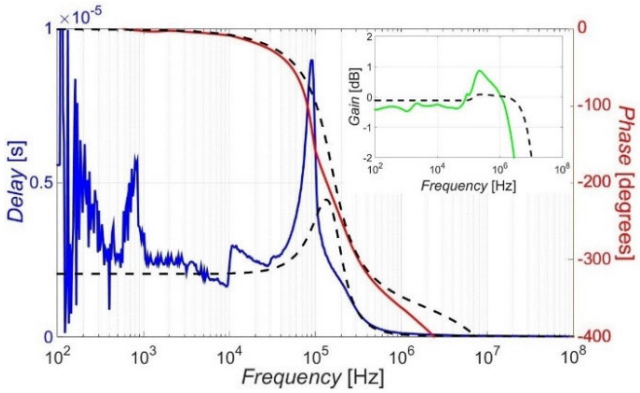

FIGURE 6. Simulation (black dashed lines) and experimental results (colored lines) of AP function.

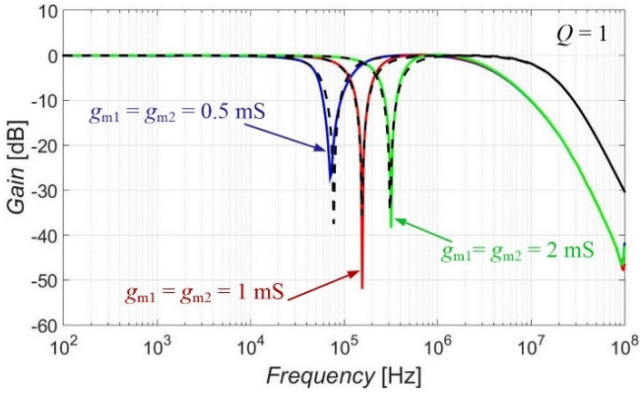

FIGURE 7. Simulation (black dashed lines) and experimental results (colored lines) of the demonstration of the electronic adjustment of the pole frequency.

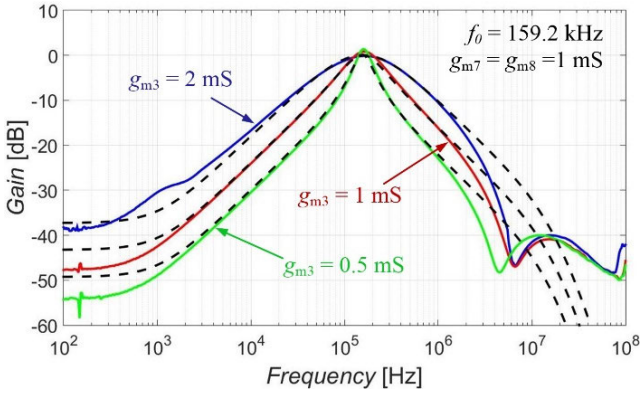

FIGURE 8. Simulation (black dashed lines) and experimental results (colored lines) of the demonstration of the electronic adjustment of the quality factor (by g_{m3}).

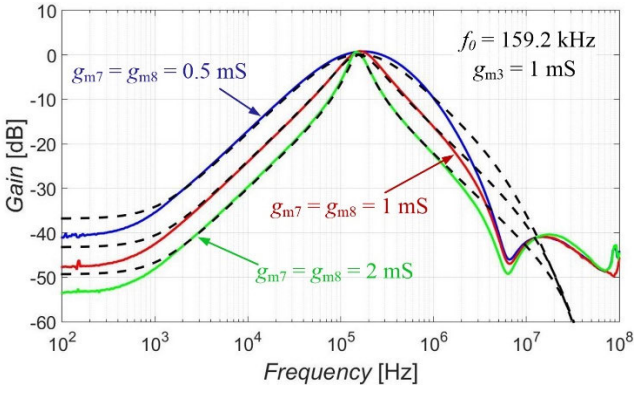

FIGURE 9. Simulation (black dashed lines) and experimental results (colored lines) of the demonstration of the electronic adjustment of the quality factor (by g_{m7} and g_{m8}).

stop–band area is affected by the leakage of the signal through the OTA when its transfer is set to 0 causing the partial addition of another term in the numerator - parasitic zero created. The PCB itself has a parasitic capacitance around 30 pF. The usable bandwidth of the filter can be widened by more suitable OTA implementation or on-chip implementation of whole filter topology.

The electronic adjustment of the pole frequency and the electronic adjustment of the quality factor were both tested for three different settings in order to demonstrate their

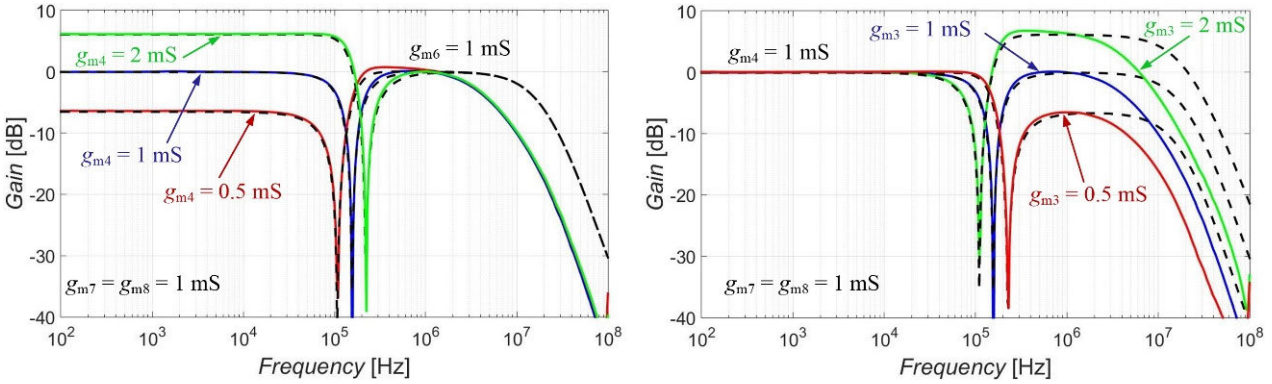

FIGURE 10. The ability to adjust the pass-band of available functions: a) adjustment of lower frequency area by change of g_{m4}, b) adjustment of higher frequency area by change of g_{m6}.

TABLE 3. Results of the electronic adjustment of the pole frequency.

$g_{m1} = g_{m2}$ [mS]	0.5	1	2
Theoretical f_0 [kHz]	79.6	159.2	318.3
Simulated f_0 [kHz]	77.6	154.5	309.0
Measured f_0 [kHz]	71.2	156.8	319.2

TABLE 4. Results of the electronic adjustment of the quality factor by gm3.

g_{m3} [mS]	2	1	0.5
Theoretical Q [-]	0.5	1	2
Simulated Q [-]	0.50	1.01	2.02
Measured Q [-]	0.51	1.10	2.32

appropriate function. The electronic adjustment of the pole frequency (independent of the quality factor) is presented on the BS function where the transconductances $g_{m1} = g_{m2}$ were set to 0.5 mS, 1 mS and 2 mS which (together with other parameters having their initial value) results in theoretical pole frequencies of 79.6 kHz, 159.2 kHz and 318.3 kHz. These results are shown in Fig. 7 and the theoretical frequencies can be compared with pole frequencies obtained from simulations and experimental measurement in Table 3. The BP function has been chosen for the demonstration of the electronic adjustment of the quality factor (independent of the pole frequency) for the setting g_{m3} being equal to 0.5 mS, 1 mS and 2 mS (while other parameters have their initial value) providing the values of the theoretical quality factor equal to 2, 1 and 0.5. The results for this feature are depicted in Fig. 8 and the theoretical values of the quality factor together with the obtained values from simulations and experimental measurement are given in Table 4. Based on Figs. 7 and 8 and Tables 3 and 4, the expected electronic tuning of pole frequency and the quality factor are both providing good results for both simulations and experimental measurement.

The quality factor of the proposed filter can be also adjusted by another way independent of the adjustment by

TABLE 5. Results of the electronic adjustment of the quality factor by gm7 and gm8.

$g_{m7} = g_{m8}$ [mS]	0.5	1	2
Theoretical Q [-]	0.5	1	2
Simulated Q [-]	0.47	1.01	2.02
Measured Q [-]	0.47	1.10	2.06

g_{m3}. This additional adjustment can be done by the change of transconductances g_{m7} and g_{m8} as long as a simple condition $g_{m7} = g_{m8}$ is fulfilled so f_0 is not affected. The values of g_{m7} and g_{m8} are set the same way as g_{m3} in the previous case (0.5 mS, 1 mS and 2 mS which results in the quality factor of 0.5, 1 and 2). Fig. 9 shows the simulation and experimental results. The theoretical, simulated and measured values of the quality factor can be compared in Table 5. The change of the gain at lower and higher frequencies cause by the change of g_{m7} and g_{m8} when adjusting Q can be easily compensated by g_{m4} and g_{m6}.

The possibility to cancel individual terms of the numerator (reconnection-less reconfiguration) can be also used (considering continuous electronic adjustment of transconductance depending on particular OTA implementation) for a beneficial feature of fine-tuning of the resulting output response. It includes the compensation of undesired gain shift of the pass-band area caused by a mismatch of individual parts/parameters or the possibility to shift the stop-band area if desired (by a partial addition of other terms which would be canceled otherwise). Fig. 10 shows the possibility to adjust the pass-band area (of available functions) at lower frequencies by the change of transconductance g_{m4} (Fig. 10a)) or at higher frequencies by the change of transconductance g_{m6} (Fig. 10b)) using the BS function for the demonstration. Similarly, the stop-band area of available functions at lower frequencies can be adjusted by changing the value of g_{m4} ($0 < g_{m4} < 1$ mS) and the stop-band area of available functions at higher frequencies can be adjusted by changing the value of g_{m6} ($0 < g_{m6} < 1$ mS).

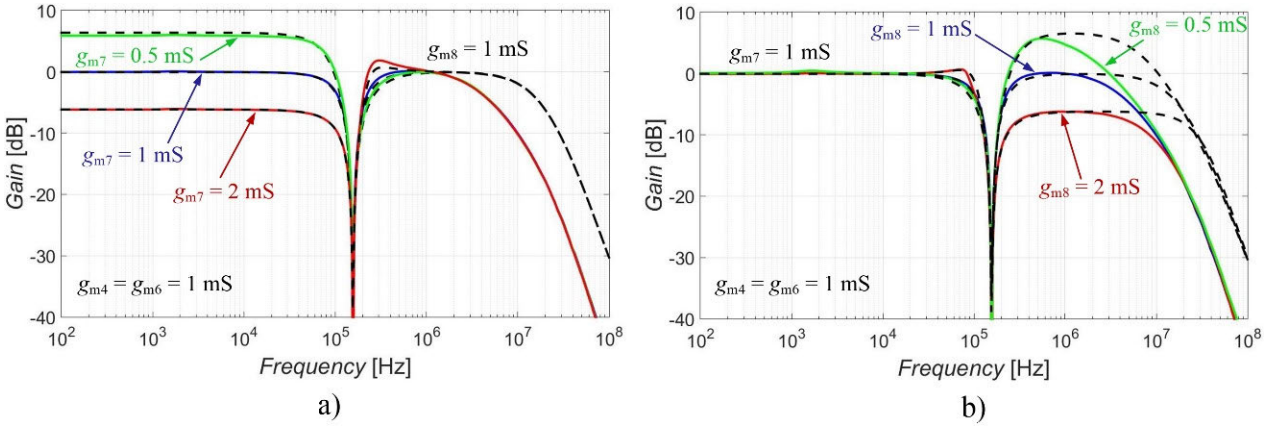

FIGURE 11. The ability to adjust the pass-band of available functions: a) adjustment of lower frequency area by change of g_{m7}, b) adjustment of higher frequency area by change of g_{m8}.

The proposed filter, due to its particular design, offers an additional possibility to adjust the pass-band area of available functions as illustrated in Fig. 11 (by using different parameters that those used for the pass-band area adjustment in Fig. 10). Analogically to the previous case, the pass-band area at lower frequencies can be adjusted by the change of transconductance g_{m7} (Fig. 11 a)) while the pass-band area at higher frequencies can be adjusted by the change of transconductance g_{m8} (Fig. 11 b)). This extends the range of adjustability of the pass-band area if one of responsible parameters (transconductances) reaches the limitations of obtainable values in dependence on particular implementation of OTA elements. In comparison to the previous case, the transconductances of g_{m7} and g_{m8} cannot be set to 0 or close to 0. It cancels (unintentionally) the terms in the denominator and changes the function of the filter or it can cause possible instability of the filter. Therefore, these parameters (g_{m7} and g_{m8}) are not suitable for the adjustment of the stop-band areas. Nonetheless, they are still fully available for the pass-band adjustment.

IV. CONCLUSION

The proposed filter has the following advantages:

a) it has both working capacitors grounded unlike other previously MUNV-based reconnection-less reconfigurable filters;
b) thanks to its specific topology and parameters forming the transfer response, the filter offers an additional electronic adjustments of the quality factor (see Figs. 8 and 9);
c) the filter offers two independent ways of the adjustment of the pass-band of available functions at lower and/or higher frequencies as demonstrated in Fig. 10 and Fig. 11.

Grounded capacitors make the proposed topology more suitable for the on-chip implementation and less sensitive to unpredictable parasitic behavior which could result in stability issues. Points b) and c) are advantages in comparison with any previously introduced low frequency reconnection-less reconfigurable filters regardless of the design approach. Two independent ways of the adjustment of the pass-band area and the quality factor bring another degree of freedom when the fine-tuning of the output response or the change of the quality factor is needed. Therefore, features and parameters of the resulting transfer function of the proposed filter extend the range of adjustability of the pass-band area and the quality factor if the tunability of the transconductance value of given implementation of the OTA element is limited (limited linearity or other limitations given by the particular relation of the resulting transconductance in dependence on driving force, for instance). The function and individual features of the proposed filter were verified by PSpice simulations using available models of used active elements and by experimental measurements using commercially available integrated circuits.

REFERENCES

[1] V. Chamnanphai and W. Sa-Ngiamvibool, "Electronically tunable SIMO mixed-mode universal filter using VDTAs," *Przegląd Elektrotechniczny*, vol. 93, no. 3, pp. 207–211, 2017, doi: 10.15199/48.2017.03.48.

[2] Y. Li, C. Wang, B. Zhu, and Z. Hu, "Universal current-mode filters based on OTA and MO-CCCA," *IETE J. Res.*, vol. 64, no. 6, pp. 897–906, Nov. 2018, doi: 10.1080/03772063.2017.1381575.

[3] P. Huaihongthong, A. Chaichana, P. Suwanjan, S. Siripongdee, W. Sunthonkanokpong, P. Supavarasuwat, W. Jaikla, and F. Khateb, "Single-input multiple-output voltage-mode shadow filter based on VDDDAs," *AEU-Int. J. Electron. Commun.*, vol. 103, pp. 13–23, May 2019, doi: 10.1016/J.AEUE.2019.02.013.

[4] U. Cini and M. Aktan, "Dual-mode OTA based biquadratic filter suitable for current-mode applications," *AEU-Int. J. Electron. Commun.*, vol. 80, pp. 43–47, Oct. 2017, doi: 10.1016/J.AEUE.2017.06.024.

[5] P. Uttaphut, "Simple three-input single-output current-mode universal filter using single VDCC," *Int. J. Electr. Comput. Eng.*, vol. 8, no. 6, pp. 4932–4940, 2018, doi: 10.11591/IJECE.V8I6.PP4932-4940.

[6] P. Mongkolwai, T. Pukkalanun, and W. Tangsrirat, "Three-input single-output current-mode biquadratic filter with high-output impedance using a single current follower transconductance amplifier," *IAENG Int. J. Comp. Sci.*, vol. 44, no. 3, pp. 383–387, 2017.

[7] M. E. Başak, "Realization of DTMOS based CFTA and multiple input single output biquadratic filter application," *AEU-Int. J. Electron. Commun.*, vol. 106, pp. 57–66, Jul. 2019, doi: 10.1016/J.AEUE.2019.04.027.

[8] M. Kumngern, F. Khateb, T. Kulej, and C. Psychalinos, "Multiple-input universal filter and quadrature oscillator using Multiple-input operational transconductance amplifiers," *IEEE Access*, vol. 9, pp. 56253–56263, 2021, doi: 10.1109/ACCESS.2021.3071829.
[9] B. J. Maundy, A. S. Elwakil, S. Ozoguz, and H. A. Yildiz, "Minimal two-transistor multifunction filter design," *Int. J. Circuit Theory Appl.*, vol. 45, no. 11, pp. 1449–1466, Nov. 2017, doi: 10.1002/CTA.2319.
[10] L. Langhammer and J. Jerabek, "Fully differential universal current-mode frequency filters based on signal-flow graphs method," *Int. J. Adv. Telecommun., Electrotech., Signals Syst.*, vol. 3, no. 1, pp. 1–12, Apr. 2014, doi: 10.11601/IJATES.V3I1.62.
[11] C.-N. Lee, "Independently tunable mixed-mode universal biquad filter with versatile input/output functions," *AEU-Int. J. Electron. Commun.*, vol. 70, no. 8, pp. 1006–1019, Aug. 2016, doi: 10.1016/J.AEUE.2016.04.006.
[12] T.-H. Lee, B. Lee, S. Nam, Y.-S. Kim, and J. Lee, "Frequency-tunable tri-function filter," *IEEE Trans. Microw. Theory Techn.*, vol. 65, no. 11, pp. 4584–4592, Nov. 2017, doi: 10.1109/TMTT.2017.2716931.
[13] E. J. Naglich, J. Lee, D. Peroulis, and W. J. Chappell, "Switchless tunable bandstop-to-all-pass reconfigurable filter," *IEEE Trans. Microw. Theory Techn.*, vol. 60, no. 5, pp. 1258–1265, May 2012, doi: 10.1109/TMTT.2012.2188723.
[14] M. Fan, K. Song, Y. Zhu, and Y. Fan, "Compact bandpass-to-bandstop reconfigurable filter with wide tuning range," *IEEE Microw. Wireless Compon. Lett.*, vol. 29, no. 3, pp. 198–200, Mar. 2019, doi: 10.1109/LMWC.2019.2892846.
[15] R. Lababidi, M. Al Shami, M. Le Roy, D. Le Jeune, K. Khoder, and A. Pérennec, "Tunable channelised bandstop passive filter using reconfigurable phase shifter," *IET Microw., Antennas Propag.*, vol. 13, no. 5, pp. 591–596, Apr. 2019, doi: 10.1049/IET-MAP.2018.5430.
[16] R. Sotner, J. Petrzela, J. Jerabek, and T. Dostal, "Reconnection-less OTA-based biquad filter with electronically reconfigurable transfers," *Elektronika Elektrotechnika*, vol. 21, no. 3, pp. 33–37, Jun. 2015, doi: 10.5755/J01.EEE.21.3.10205.
[17] R. Sotner, J. Petrzela, J. Jerabek, K. Vrba, and T. Dostal, "Solutions of reconnection-less OTA-based biquads with electronical transfer response reconfiguration," in *Proc. 25th Int. Conf. Radioelektronika*. Apr. 2015, pp. 40–45, doi: 10.1109/RADIOELEK.2015.7128991.
[18] L. Langhammer, R. Sotner, and T. Dostal, "New solution of a frequency filter with reconnection-less reconfiguration of its transfer," in *Proc. 29th Int. Conf. Radioelektronika*, Pardubice, Czech Republic, Apr. 2019, pp. 51–54, doi: 10.1109/RADIOELEK.2019.8733544.
[19] L. Langhammer, R. Sotner, J. Dvorak, J. Jerabek, and P. A. Ushakov, "Novel reconnection-less reconfigurable filter design based on unknown nodal voltages method and its fractional-order counterpart," *Elektronika Elektrotechnika*, vol. 25, no. 3, pp. 34–38, Jun. 2019, doi: 10.5755/J01.EIE.25.3.23673.
[20] L. Langhammer, R. Sotner, J. Dvorak, and T. Dostal, "Dual-mode multifunctional reconnection-less reconfigurable filter," *Elektronika Elektrotechnika*, vol. 26, no. 3, pp. 36–41, Jun. 2020, doi: 10.5755/J01.EIE.26.3.25856.
[21] L. Langhammer, J. Dvorak, R. Sotner, J. Jerabek, and P. Bertsias, "Reconnection–less reconfigurable low–pass filtering topology suitable for higher–order fractional–order design," *J. Adv. Res.*, vol. 25, pp. 257–274, Sep. 2020, doi: 10.1016/J.JARE.2020.06.022.
[22] P. R. Gray, P. J. Hurst, S. H. Lewis, and R. G. Meyer, *Analysis and Design of Analog Integrated Circuits*. Hoboken, NJ, USA: Wiley, 2009, p. 896.
[23] N. S. Nise, "Signal-flow graphs," in *The Control Handbook*. Piscataway, NJ, USA: IEEE Press, 1996.
[24] S. Mason, "Feedback theory-some properties of signal flow graphs," *Proc. IRE*, vol. 41, no. 9, pp. 1144–1156, Sep. 1953, doi: 10.1109/JRPROC.1953.274449.
[25] C. Coates, "Flow-graph solutions of linear algebraic equations," *IRE Trans. Circuit Theory*, vol. 6, no. 2, pp. 170–187, 1959, doi: 10.1109/TCT.1959.1086537.
[26] W. K. Chen, *The Circuits and Filters Handbook*, 3rd ed. Boca Raton, FL, USA: CRC Press, 2009.
[27] D. Biolek, R. Senani, V. Biolkova, and Z. Kolka, "Active elements for analog signal processing: Classification, review, and new proposals," *Radioengineering*, vol. 17, no. 4, pp. 15–32, Dec. 2008.
[28] Linear Technology. (2012). *LT1228 Current Feedback Amplifier With DC Gain Control (Datasheet)*. Accessed: Oct. 12, 2022. [Online]. Available: http://cds.linear.com/docs/en/datasheet/1228fd.pdf

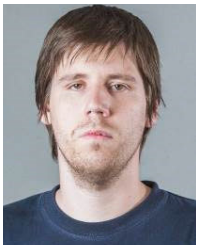

LUKAS LANGHAMMER received the M.Sc. and Ph.D. degrees in electrical engineering and telecommunication from the Faculty of Electrical Engineering and Communication, Brno University of Technology (BUT), Brno, Czech Republic, in 2012 and 2016, respectively.

He is currently working with the Department of Electrical Engineering, Faculty of Military Technology, University of Defence, Brno, and also with the Department of Telecommunications, Faculty of Electrical Engineering and Communication, BUT. His research interests include design and analysis of frequency filters, basic analog building blocks, and advanced active elements.

ROMAN SOTNER (Member, IEEE) was born in Znojmo, Czech Republic, in 1983. He received the M.Sc. and Ph.D. degrees in electrical engineering from the Brno University of Technology (BUT), Czech Republic, in 2008 and 2012, respectively.

He is currently an Associate Professor with the Department of Radio Electronics, Faculty of Electrical Engineering and Communication, BUT. His research interests include discrete as well as integrated analogue circuits (active filters, oscillators, and audio), circuits in the current mode, circuits with direct electronic controlling possibilities especially, analog signal processing in sensing applications, and computer simulation.